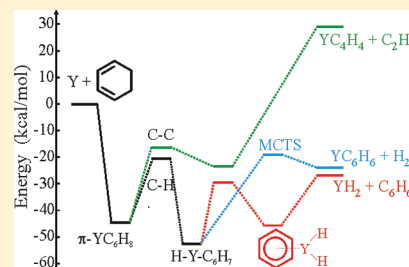


Reactions of Neutral Gas-Phase Yttrium Atoms with Two Cyclohexadiene Isomers

Jonathan J. Schroden and H. Floyd Davis*

Department of Chemistry and Chemical Biology, Cornell University, Ithaca, New York 14853, United States

ABSTRACT: The reactions of neutral ground-state yttrium (Y) atoms with 1,3- and 1,4-cyclohexadiene (CHD) were studied using crossed molecular beams. Formation of $YC_6H_6 + H_2$ and $YH_2 + C_6H_6$ was observed for both isomers at collision energies (E_{coll}) of 31.3 and 13.0 kcal/mol. Measured product branching ratios at $E_{coll} = 31.3$ kcal/mol indicated that $YH_2 + C_6H_6$ was the dominant channel, accounting for >97% of the products. An additional minor product channel, $YC_4H_4 + C_2H_4$, was observed for 1,3-CHD at the higher E_{coll} . The reaction threshold for YC_4H_4 formation was determined to be 29.5 ± 2.0 kcal/mol based on fits to the data.



I. INTRODUCTION

The reactions of neutral gas-phase transition-metal atoms with hydrocarbons have been an active area of study due to their ability to act as simple models for reactions important in catalysis. Much of the earliest experimental work focused on the smallest saturated hydrocarbons, namely, methane^{1–5} and ethane,^{2,5,6} but several larger (and unsaturated) hydrocarbons have also been studied.^{7–11} We have studied reactions of ethylene,¹¹ acetylene,¹¹ cyclopropane,¹² propene,¹² four butene isomers,¹³ propyne,¹⁴ and 2-butyne.¹⁴ In our studies of the methane and ethane reactions, only products from cleavage of C–H bonds were observed,^{5,6} while reactions with the larger hydrocarbons also yielded product channels resulting from cleavage of C–C bonds.^{12–14} Experimentally measured branching ratios for these reactions have, in some cases, shown the C–C bond cleavage products to be dominant.^{12a}

In the current study, we look at reactions of yttrium, the simplest second-row transition-metal atom, with 1,3- and 1,4-cyclohexadiene (CHD), thereby extending the size of the hydrocarbon reactant to six carbons. These reactions have not been studied previously, although there have been studies involving niobium clusters,¹⁵ aluminum atoms,¹⁶ and metal cations.¹⁷ Also, photodissociation of 1,4-CHD leading to H_2 elimination has been studied.¹⁸ On the basis of available binding energies^{19,20} and heats of formation,²¹ a schematic reaction coordinate for the Y + 1,3-CHD reaction can be drawn (Figure 1).²² Two possible product channels, corresponding to elimination of H_2 and C_6H_6 , should be exoergic. A third reactive channel, corresponding to elimination of C_2H_4 , may also be accessible, particularly at higher collision energies. There have been no previous computational studies of the reactions of transition-metal atoms with 1,3- and 1,4-CHD.

II. EXPERIMENTAL SECTION

The experiments were conducted using a rotatable source crossed molecular beams apparatus.²³ The 532 nm output (10 mJ/pulse) of a Nd:YAG laser (Continuum Surelite) operating at 30 Hz was focused onto a 0.25-in. diameter yttrium rod (Alfa

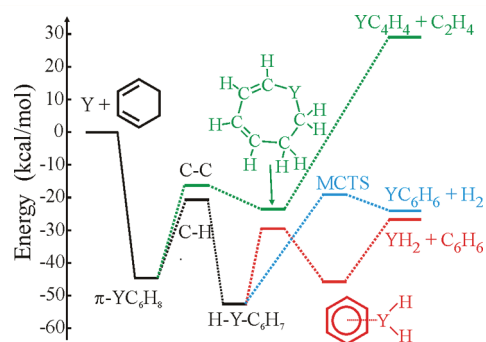


Figure 1. Schematic potential energy diagram for the Y + 1,3-CHD reaction. Product thermodynamics were calculated based on known binding energies^{19,20} and heats of formation.^{21,22} Other stationary points are estimated by analogy to other Y reactions. A possible second mechanism for YC_4H_4 formation involving concerted elimination of C_2H_4 from the π -complex has been omitted for the sake of clarity.

Aesar, 99% purity). The ablated yttrium atoms were subsequently entrained in a supersonic inert gas pulse^{23,24} (He or Ne, 5 psig), forming the metal beam that was then skimmed, collimated, and chopped by a slotted chopper wheel spun at 210 Hz. The CHD beams were generated by passing an inert carrier gas (He, 5 psig) through a glass bubbler containing pure liquid 1,3- or 1,4-CHD (Aldrich) held at room temperature. The resulting mixture was sent to a second pulsed valve. The CHD beams were also skimmed before crossing the yttrium beam at 90°. Electron impact ionization was used to measure the velocity distributions of both beams, using the time-of-flight (TOF) method.²³ Parameters relevant to the beam profiles are given in Tables 1 and 2. The yttrium beam has been shown to consist only of two spin-orbit states of the ground electronic state, $Y(a^2D_{3/2})$ and $Y(a^2D_{5/2})$.^{11b}

Received: December 6, 2011

Revised: March 13, 2012

Published: April 2, 2012

Table 1. Experimental Conditions for Y + 1,3-CHD Reactions

E_{coll}^a	Y carrier gas	Y beam velocity ^b	Y beam fwhm ^b	1,3-CHD temperature	1,3-CHD beam velocity ^b	1,3-CHD beam fwhm ^b
13.0	Ne	1090	150	room temp.	1183	104
31.3	He	2180	261	room temp.	1183	104

^aUnits: kcal/mol. ^bUnits: m/s.**Table 2. Experimental Conditions for Y + 1,4-CHD Reactions**

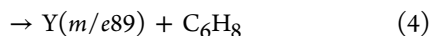
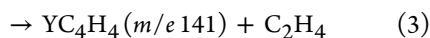
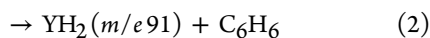
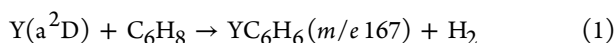
E_{coll}^a	Y carrier gas	Y beam velocity ^b	Y beam fwhm ^b	1,4-CHD temperature	1,4-CHD beam velocity ^b	1,4-CHD beam fwhm ^b
13.0	Ne	1090	150	room temp.	1280	106
31.3	He	2180	261	room temp.	1280	106

^aUnits: kcal/mol. ^bUnits: m/s.

Yttrium-containing products from reactive and nonreactive collisions drifted 24.1 cm to the detector, where they were ionized at 157 nm using a F₂ excimer laser (~1 mJ/pulse).²³ By scanning the delay time of the excimer trigger with respect to a time zero for reaction, product TOF spectra were obtained. Integration of these spectra at different angles yielded the lab angular distribution, $N(\Theta)$. Using a forward-convolution program with instrumental and experimental parameter inputs (aperture sizes, flight distances, beam velocities, etc.), along with two center-of-mass (CM) input functions (the translational energy release distribution, $P(E)$, and the CM angular distribution, $T(\theta)$), TOF spectra and lab angular distributions were calculated and compared with experimental data. The two CM functions were iteratively adjusted until calculated angular distributions and TOF spectra matched those from experiment.

III. RESULTS

A. $E_{\text{coll}} = 31.3$ kcal/mol. Reactions of neutral yttrium atoms with 1,3- and 1,4-CHD at $E_{\text{coll}} = 31.3$ kcal/mol resulted in signal at four m/e ratios



A Newton diagram²⁵ in velocity space is shown in Figure 2 for the Y + 1,3-CHD reaction. The rings (Newton circles) correspond to the maximum range of scattering for each product, assuming that all available energy (E_{avail}) is channeled into translational energy. These circles were calculated using the thermodynamics shown in Figure 1, along with conservation of energy and linear momentum. Although the $\text{YC}_6\text{H}_6 + \text{H}_2$ channel is quite exothermic, because of the light counterfragment (H_2), linear momentum conservation constrains the YC_6H_6 products to a small range of lab angles. The YH_2 products recoil from a much heavier counterfragment (C_6H_6), enabling them to scatter over a very wide range of lab angles. The $\text{YC}_4\text{H}_4 + \text{C}_2\text{H}_4$ channel is substantially endoergic, making the YC_4H_4 constrained to a very small range of laboratory angles.

Laboratory TOF spectra for the YC_6H_6 , YH_2 , and YC_4H_4 products from the Y + 1,3-CHD reaction at $E_{\text{coll}} = 31.3$ kcal/

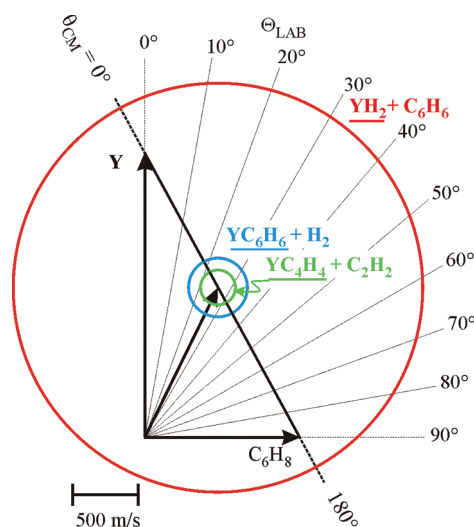


Figure 2. Newton diagram in velocity space for the Y + 1,3-CHD reaction at $E_{\text{coll}} = 31.3$ kcal/mol. Circles represent the maximum CM velocity constraints on the indicated metal-containing fragment from the various product channels based on reaction thermodynamics as shown in Figure 1 and momentum conservation.

mol are shown in Figures 3–5, respectively. Spectra for the YC_6H_6 and YH_2 product channels from the reaction with 1,4-

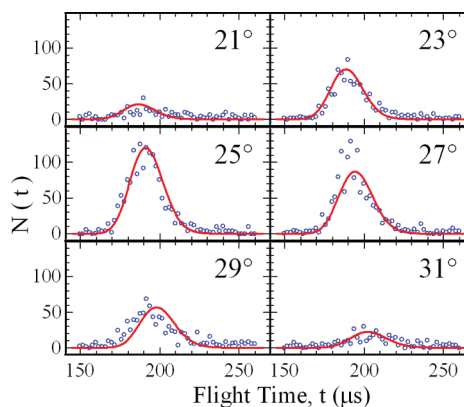


Figure 3. Sample TOF spectra at indicated lab angles for YC_6H_6 products from the 1,3-CHD reaction at $E_{\text{coll}} = 31.3$ kcal/mol. Solid-line fits are generated using CM distributions shown in Figure 7.

CHD look quite similar to those shown in Figures 3 and 4, respectively, and are not shown. Upon inspection of the m/e 141 (YC_4H_4^+) data from 1,4-CHD, it was evident that the TOFs and lab angular distribution were identical to those for the YC_6H_6 products, but at 6.5% of the signal intensity. It was concluded that the signal at m/e 141 from 1,4-CHD was actually due to fragmentation of the YC_6H_6 product channel, rather than genuine YC_4H_4 reactive signal. Accordingly, 6.5% of the YC_6H_6 signal has been subtracted from the YC_4H_4 data for 1,3-CHD as well. The lab angular distributions for the reactive product channels from both isomers are shown in Figure 6.

The solid-line fits shown in Figures 3–6 were generated using the CM distributions shown in Figure 7. The YC_6H_6 and YH_2 data for both 1,3- and 1,4-CHD could be fit using the same CM distributions. The translational energy distributions, $P(E)$, for YC_6H_6 and YH_2 products peaked slightly away from zero, with $\langle P(E) \rangle = 4.97$ and 8.83 kcal/mol, respectively. Using the thermodynamics shown in Figure 1, one can calculate the

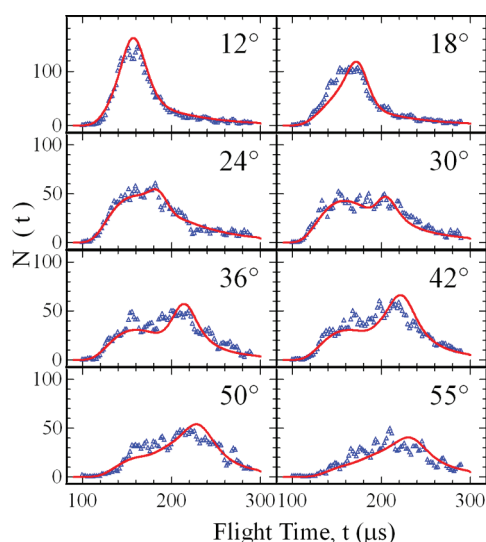


Figure 4. Sample TOF spectra at indicated lab angles for YH_2 products from the 1,3-CHD reaction at $E_{\text{coll}} = 31.3$ kcal/mol. Solid-line fits are generated using the CM distributions shown in Figure 7.

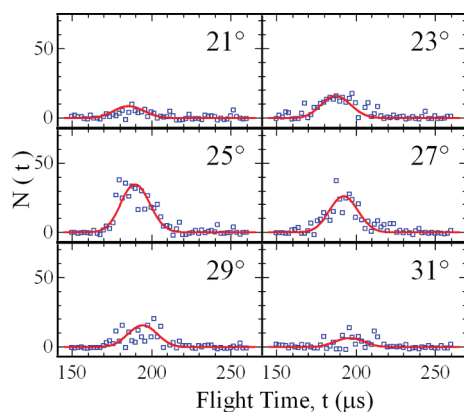


Figure 5. Sample TOF spectra at indicated lab angles for YC_4H_4 products from the 1,3-CHD reaction at $E_{\text{coll}} = 31.3$ kcal/mol. Solid-line fits are generated using CM distributions shown in Figure 7.

average fraction of E_{avail} appearing as translational energy to be $\langle f_{\text{T}} \rangle = 0.089$ and 0.152 for YC_6H_6 and YH_2 products, respectively. The $P(E)$ for YC_4H_4 products peaked very close to the zero of translational energy, with $\langle P(E) \rangle = 0.32$ kcal/mol, and only extended to 1.5 kcal/mol. The CM angular distribution, $T(\theta)$, for YC_6H_6 products was isotropic.²⁶ The $T(\theta)$ for YH_2 products was quite strongly peaked in the forward and backward directions ($\theta = 0^\circ$ and 180° , respectively), with $T(0^\circ)/T(90^\circ) = 6.32$. The $T(\theta)$ for YC_4H_4 products was slightly forward–backward peaked, with $T(0^\circ)/T(90^\circ) = 2.00$.

In order to fit the widths and arrival times of the TOF spectra for the YC_4H_4 products from the 1,3-CHD reaction, it was necessary to assume a reaction threshold of 29.5 ± 2.0 kcal/mol.²⁷ This threshold corresponds to a step-like cutoff, such that any reactants with a collision energy below this threshold cannot lead to products. More will be said about this shortly.

Determination of the branching ratios for the competing reactive channels required consideration of the photoionization cross sections, fragmentation patterns, and Jacobian factors for each reaction. In this study, the product fragmentation patterns

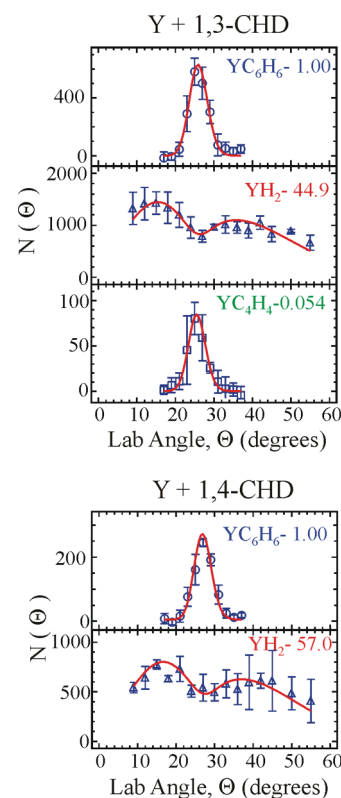


Figure 6. Lab angular distributions for all reactive product channels from the reaction of Y with both CHD isomers at $E_{\text{coll}} = 31.3$ kcal/mol. Products are, from top to bottom, YC_6H_6 (open circles), YH_2 (open triangles), and YC_4H_4 (open squares). Solid-line fits are generated using CM distributions shown in Figure 7. Corresponding product yields are indicated in the upper-right corner of each graph. Each distribution is scaled to the same number of scans (2).

and Jacobian factors were explicitly included in the analysis. The photoionization cross sections were assumed to be identical for each product.¹² The branching ratios were $\phi_{\text{YC}_6\text{H}_6}/\phi_{\text{YH}_2}/\phi_{\text{YC}_4\text{H}_4} = 1.00:44.9:0.054$ for 1,3-CHD and $\phi_{\text{YC}_6\text{H}_6}/\phi_{\text{YH}_2}/\phi_{\text{YC}_4\text{H}_4} = 1.00:57.0:0.00$ for 1,4-CHD (upper-right corners of Figure 6). Thus, the reaction forming $\text{YH}_2 + \text{C}_6\text{H}_6$ was by far the dominant process at $E_{\text{coll}} = 31.3$ kcal/mol, accounting for $>97\%$ of the products from reactions of both CHD isomers.

B. $E_{\text{coll}} = 13.0$ kcal/mol. The reactions of Y with 1,3- and 1,4-CHD were also studied at a collision energy of 13.0 kcal/mol. Only YC_6H_6 and YH_2 products were observed at the CM angle for both isomers, in addition to nonreactive scattering. The signal for both reactive products was too weak at this collision energy to allow full data sets to be taken.

IV. DISCUSSION

Because there have been no electronic structure calculations carried out on the reaction of yttrium with either CHD isomer, the thermodynamics and barrier heights must be estimated from similar systems studied previously. All of the reactive scattering channels for both isomers exhibited CM angular distributions with forward–backward symmetry, indicating that the reaction coordinates contain at least one intermediate that is long-lived with respect to its picosecond rotational period.²⁶ This is consistent with a mechanism that involves initial formation of a donor–acceptor complex between Y and the π -bonds of CHD. As shown in Figure 1, following π -complex

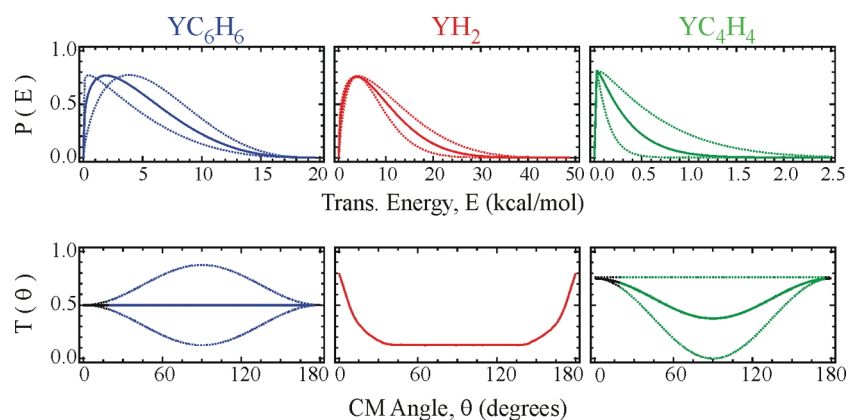


Figure 7. CM distributions used to fit TOF data for YC_6H_6 , YH_2 , and YC_4H_4 products shown in Figures 3–5, respectively, as well as for lab angular distributions shown in Figure 6. Dashed lines correspond to the range of distributions that give acceptable fits to the data.

formation, there is possibly a competition between C–H and C–C bond insertion. Insertion into a C–H bond yields H–Y– C_6H_7 . This complex can undergo H migration to give a (H)(H)Y(C_6H_6) intermediate that can decay to form $YH_2 + C_6H_6$. In previous studies of Y atom reactions with C_2H_6 ⁶ and H_2CO ,^{28–30} YH_2 was found to be the dominant product, as is the case in the present study. This behavior, which has been discussed in considerable detail previously, is a consequence of the fact that H atom migration following C–H insertion is facile in these systems, producing LYH_2 ($L = C_2H_4$ or CO).^{6,29} The same situation is expected in the present case, where $L = C_6H_6$. Unimolecular decomposition by simple loss of L from LYH_2 proceeds with little or no potential energy barrier in excess of the reaction endoergicity. Note that because LYH_2 is a true dihydride with metal hydrogen bonds (rather than a $\sigma-H_2$ complex) and because of the limited capacity for Y to undergo multicenter bonding (due to the presence of only three valence electrons), H_2 elimination from LYH_2 will encounter significant potential energy barriers and is not expected to be competitive with L loss. Instead, the most dynamically favorable mechanism for H_2 elimination starts from the H–Y– C_6H_7 complex followed by H migration to the H atom attached to yttrium (rather to Y), subsequently eliminating H_2 over a multicentered transition state (MCTS).^{9b,30}

The CM angular distributions for the different product channels observed in this study are quite similar to those reported earlier in studies of $Y + C_2H_6$ ⁶ and $Y + H_2CO$.^{28,29} The forward–backward symmetry in $T(\Theta)$ has been observed in nearly all transition-metal hydrocarbon reactions studied to date, and, as already noted, is a direct consequence of one or more reaction intermediates having lifetimes exceeding their rotational periods.^{25,26} For the $YH_2 + C_6H_6$ channel, the sharp peaking of $T(\Theta)$ at $\Theta = 0$ and 180° is a consequence of angular momentum conservation in a reaction where product rotational excitation is small.^{6,28,29} In contrast, the isotropic nature of the $T(\Theta)$ for the H_2 elimination channels results from the significant angular momentum constraints imposed by the small product reduced mass μ . In this case, the exit orbital angular momentum, $L' = \mu vb'$ (where b' is the exit impact parameter) is constrained to be much smaller than the total angular momentum of the reaction intermediate; therefore, a substantial fraction of angular momentum must be channeled into rotational angular momentum of the products, leading to an essentially isotropic $T(\Theta)$.^{6,28}

Insertion of Y into a C–C bond of CHD is also possible, leading to a seven-member ring intermediate (Figure 8), which

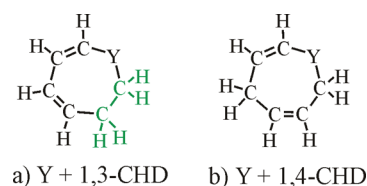


Figure 8. Schematic structures for the C–C insertion intermediate from the (a) 1,3-CHD and (b) 1,4-CHD reactions.

could subsequently undergo intramolecular rearrangement and dissociate to form $YC_4H_4 + C_2H_4$. It is quite interesting that C_2H_4 elimination is observed for 1,3-CHD but not for 1,4-CHD. Analysis of the seven-member ring intermediates formed upon C–C insertion for each of the two isomers (Figure 8) shows that for 1,3-CHD, elimination of ethylene requires very little molecular rearrangement because there is essentially an ethylene moiety already present in the ring (Figure 8a). Elimination of ethylene from the seven-member ring formed upon C–C insertion for 1,4-CHD would require substantial rearrangement because the carbons with two hydrogens attached are now no longer adjacent to one another (Figure 8b).

It is also possible that for 1,3-CHD, the $YC_4H_4 + C_2H_4$ products are formed directly from the π -complex and via concerted elimination of C_2H_4 with concurrent formation of a metallocyclopentadiene complex (see below). In this case, the reaction occurs without explicit insertion of Y into a C–C bond, as has been proposed for other large hydrocarbons.^{12–14} On the basis of our experimental data, it is not possible to determine whether C_2H_4 elimination involves a concerted process directly from the π -complex or from a C–C insertion intermediate. Theoretical calculations would be very valuable in this regard.

Elimination of molecular hydrogen from either CHD isomer should result in formation of a YC_6H_6 complex. Although the binding energy of Y to C_6H_6 (benzene) is not known, the binding energies of benzene to several first-row transition-metal atoms have been determined.¹⁹ In constructing Figure 1, a binding energy of 19.5 kcal/mol was assumed for Y.³¹ Using this value, formation of YC_6H_6 should be exoergic (–24.7 kcal/mol). It is interesting that despite the large amount of available energy for the YC_6H_6 products ($E_{avail} = 56.0$ kcal/mol at $E_{coll} =$

31.3 kcal/mol), a relatively small fraction ($\langle f_T \rangle = 0.089$) is deposited into translational energy. This is most likely due to the large number of vibrational degrees of freedom of the YC_6H_6 complex. On the basis of energetic considerations of C_6H_6 isomers,³² the counterfragment to formation of YH_2 is benzene, which makes this product channel quite exoergic as well (-26.8 kcal/mol). Again, there is a relatively small fraction of the E_{avail} appearing in translation ($\langle f_T \rangle = 0.152$), presumably due to the large number of vibrational modes of benzene.

As mentioned above, it was necessary to include a reaction threshold of 29.5 kcal/mol in order to accurately fit the YC_4H_4 data from 1,3-CHD. Without detailed ab initio calculations, it is difficult to say to what this threshold corresponds with absolute certainty. However, consideration of possible product structures may help in this regard. Figure 9 shows four possible

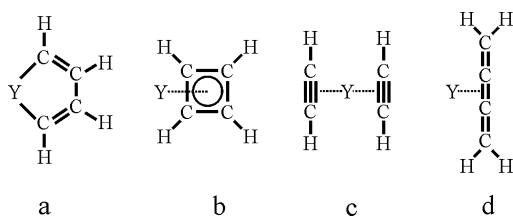


Figure 9. Schematic structures for possible YC_4H_4 products from the 1,3-CHD reaction: (a) metallacyclopentadiene, (b) Y-cyclobutadiene, (c) $Y-(C_2H_2)_2$, and (d) Y-butatriene.

product structures for YC_4H_4 , corresponding to a metallacyclopentadiene (Figure 9a), a Y-cyclobutadiene complex (Figure 9b), a $Y-(C_2H_2)_2$ complex (Figure 9c), and a Y-butatriene complex (Figure 9d). If we take the measured threshold to be the reaction endoergicity, we can use known heats of formation²¹ to determine the bond energies of Y in each complex. For the metallacyclopentadiene complex, each Y-C bond would have $D_0 = 75.0$ kcal/mol, while the Y-cyclobutadiene complex would be bound by 60 kcal/mol. For the $Y-(C_2H_2)_2$ complex, assuming that the first acetylene moiety is bound by 48.6 kcal/mol³³ gives $D_0 = 17.8$ kcal/mol for the second acetylene unit. Finally, the Y-butatriene complex would be bound by 41.0 kcal/mol.

Although we cannot explicitly rule out any of these structures based on our data, we can make arguments against some of them. The $Y-(C_2H_2)_2$ complex seems unlikely for three reasons. First, assuming that the reaction threshold corresponds to the endoergicity leaves the second acetylene unit bound by only 17.8 kcal/mol, which seems weak for a $Y-(C\equiv C)$ bond. Second, formation of this product requires cleavage of an additional C-C bond, a requirement not shared by the other structures. Third, it seems likely based on our past experience¹⁴ that a $Y-(C_2H_2)_2$ complex would fragment upon ionization to form $Y(C_2H_2)^+ + C_2H_2$, but the fragmentation pattern for $Y + 1,3-CHD$ showed no signal at m/e 115 ($YC_2H_2^+$). The Y-butatriene complex seems unlikely because taking the reaction endoergicity to be 29.5 kcal/mol makes this complex bound by 41.0 kcal/mol, which seems large compared to the 28.0 kcal/mol binding energy calculated for the $Y-C_2H_4$ complex.^{8b} The Y-cyclobutadiene structure seems quite unlikely because cyclobutadiene is antiaromatic. It therefore seems that the metallacyclopentadiene structure is the most likely candidate. Assuming 29.5 kcal/mol to be the reaction endoergicity yields reasonable bond energies for this structure, and its formation

requires the least amount of molecular rearrangement from either the seven-member ring intermediate or the π -complex.

If the metallacyclopentadiene is formed via the stepwise C-C insertion mechanism (Figure 1), the equation of the measured reaction threshold to the reaction endoergicity seems reasonable because the dissociating intermediate would have a structure similar to that shown in Figure 9a but with an additional C_2H_4 unit bonded to yttrium. The final dissociation step would then be simple bond fission and loss of C_2H_4 , which should proceed without a barrier in excess of the reaction endoergicity. If, on the other hand, the dominant mechanism is one involving concerted loss of C_2H_4 from the initially formed π -complex, the measured reaction threshold may correspond to a MCTS that lies above the reaction endoergicity. Detailed ab initio calculations would be useful in providing more insight into the reaction mechanism(s) for production of $YC_4H_4 + C_2H_4$.

V. CONCLUSION

The reactions of neutral yttrium atoms with 1,3- and 1,4-CHD were studied at two different collision energies. At the higher collision energy, formation of YC_6H_6 , YH_2 , and nonreactive scattering was observed for both isomers. An additional product channel, forming YC_4H_4 , was observed only for 1,3-CHD. At the lower collision energy, only YC_6H_6 , YH_2 , and nonreactive scattering products were observed for both isomers. A mechanism for formation of YC_6H_6 and YH_2 is proposed involving initial π -complex formation followed by insertion of Y into a C-H bond. Subsequent H migration steps lead to these two product channels. Two possible mechanisms for YC_4H_4 formation are discussed, corresponding to formation of a π -complex followed by either concerted C_2H_4 loss or insertion of Y into a C-C bond to form a seven-member ring intermediate that subsequently undergoes intramolecular rearrangement to form $YC_4H_4 + C_2H_4$. Several possible structures are considered for the YC_4H_4 product, with the most likely corresponding to a metallacyclopentadiene complex. A reaction threshold of 29.5 ± 2.0 kcal/mol was measured for this product channel, which may correspond to the reaction endoergicity or a MCTS above the product asymptote, depending on the mechanism of YC_4H_4 formation.

■ AUTHOR INFORMATION

Corresponding Author

*E-mail: hfd1@cornell.edu.

Notes

The authors declare no competing financial interest.

■ ACKNOWLEDGMENTS

This work was supported by the National Science Foundation, Grant Number CHE-0809622. We thank Chia Chen Wang for valuable assistance with the early experiments on these systems.

■ REFERENCES

- (1) Parnis, J. M.; Lafleur, R. D.; Rayner, D. M. *J. Phys. Chem.* **1995**, *99*, 673–680.
- (2) Senba, K.; Matsui, R.; Honma, K. *J. Phys. Chem.* **1995**, *99*, 13992–13999.
- (3) (a) Campbell, M. L. *J. Am. Chem. Soc.* **1997**, *119*, 5984–5985. (b) Campbell, M. L. *J. Phys. Chem. A* **1997**, *101*, 9377–9381. (c) Campbell, M. L. *J. Phys. Chem. A* **1998**, *102*, 892–896. (d) Campbell, M. L. *J. Chem. Soc., Faraday Trans.* **1998**, *94*, 353–358. (e) Campbell, M. L. *Chem. Phys. Lett.* **2002**, *365*, 361–365.

- (4) Willis, P. A.; Stauffer, H. U.; Hinrichs, R. Z.; Davis, H. F. *J. Chem. Phys.* **1998**, *108*, 2665–2668.
- (5) Hinrichs, R. Z.; Willis, P. A.; Stauffer, H. U.; Schroden, J. J.; Davis, H. F. *J. Chem. Phys.* **2000**, *112*, 4634–4643.
- (6) Stauffer, H. U.; Hinrichs, R. Z.; Schroden, J. J.; Davis, H. F. *J. Phys. Chem. A* **2000**, *104*, 1107–1116.
- (7) Weisshaar, J. C. *Acc. Chem. Res.* **1993**, *26*, 213–219.
- (8) (a) Carroll, J. J.; Weisshaar, J. C.; Siegbahn, P. E. M.; Wittborn, C. A. M.; Blomberg, M. R. A. *J. Phys. Chem.* **1995**, *99*, 14388–14396. (b) Carroll, J. J.; Haug, K. L.; Weisshaar, J. C.; Blomberg, M. R. A.; Siegbahn, P. E. M.; Svensson, M. *J. Phys. Chem.* **1995**, *99*, 13955–13969.
- (9) (a) Porembski, M.; Weisshaar, J. C. *J. Phys. Chem. A* **2001**, *105*, 4851–4864. (b) Porembski, M.; Weisshaar, J. C. *J. Phys. Chem. A* **2001**, *105*, 6655–6667. (c) Porembski, M.; Weisshaar, J. C. *J. Phys. Chem. A* **2000**, *104*, 1524–1531.
- (10) (a) Mitchell, S. A.; Hackett, P. A.; Rayner, D. M.; Cantin, M. J. *J. Phys. Chem.* **1986**, *90*, 6148–6154. (b) Blitz, M. A.; Mitchell, S. A.; Hackett, P. A. *J. Phys. Chem.* **1991**, *95*, 8719–8726. (c) Mitchell, S. A.; Blitz, M. A.; Fournier, R. *Can. J. Chem.* **1994**, *72*, 587–599. (d) Lian, L.; Mitchell, S. A.; Rayner, D. M. *J. Phys. Chem.* **1994**, *98*, 11637–11647.
- (11) (a) Willis, P. A.; Stauffer, H. U.; Hinrichs, R. Z.; Davis, H. F. *J. Phys. Chem. A* **1999**, *103*, 3706–3720. (b) Stauffer, H. U.; Hinrichs, R. Z.; Willis, P. A.; Davis, H. F. *J. Chem. Phys.* **1999**, *111*, 4101–4112.
- (12) (a) Hinrichs, R. Z.; Schroden, J. J.; Davis, H. F. *J. Am. Chem. Soc.* **2003**, *125*, 860–861. (b) Hinrichs, R. Z.; Schroden, J. J.; Davis, H. F. *J. Phys. Chem. A* **2003**, *107*, 9284–9294.
- (13) Schroden, J. J.; Wang, C. C.; Davis, H. F. *J. Phys. Chem. A* **2003**, *107*, 9295–9300.
- (14) Hinrichs, R. Z.; Schroden, J. J.; Davis, H. F. *J. Phys. Chem. A* **2008**, *112*, 3010–3019.
- (15) St. Pierre, R. J.; Chronister, E. L.; Song, L.; El-Sayed, M. A. *J. Phys. Chem.* **1987**, *91*, 4648–4651.
- (16) Mitchell, S. A.; Simard, B.; Rayner, D. M.; Hackett, P. A. *J. Phys. Chem.* **1988**, *92*, 1655–1664.
- (17) (a) Cornehl, H. H.; Heinemann, C.; Schroder, D.; Schwarz, H. *Organometallics* **1995**, *14*, 992–999. (b) Schroeter, K.; Schalley, C. A.; Wesendrup, R.; Schroder, D.; Schwarz, H. *Organometallics* **1997**, *16*, 986–994.
- (18) Zhao, X.; Continetti, R. E.; Yokoyama, A.; Hints, E. J.; Lee, Y. T. *J. Chem. Phys.* **1989**, *91*, 4118–4127.
- (19) Kurikawa, T.; Takeda, H.; Hirano, M.; Judai, K.; Arita, T.; Nagao, S.; Nakajima, A.; Kaya, K. *Organometallics* **1999**, *18*, 1430–1438.
- (20) Siegbahn, P. E. M. *Theor. Chim. Acta* **1994**, *87*, 441–452.
- (21) (a) Zahradnik, R.; Hobza, P.; Burcl, R.; Hess, B. A. Jr.; Radziszewski, J. G. *J. Mol. Struct.: THEOCHEM* **1994**, *313*, 335–349. (b) Wang, H.; Brezinsky, K. *J. Phys. Chem. A* **1998**, *102*, 1530–1541. (c) Thermodynamics Research Center, NIST Boulder Laboratories. Thermodynamics Source Database. In *NIST Chemistry WebBook*, NIST Standard Reference Database Number 69; Linstrom, P. J., Mallard, W. G., Eds.; National Institute of Standards and Technology: Gaithersburg MD, July 2001; <http://webbook.nist.gov>.
- (22) Note that the heats of formation for 1,3- and 1,4-CHD are nearly identical; therefore, the product asymptotes in Figure 1 should be the same for the reaction of Y with both isomers. The values of other stationary points may differ due to different bonding interactions.
- (23) Willis, P. A.; Stauffer, H. U.; Hinrichs, R. Z.; Davis, H. F. *Rev. Sci. Instrum.* **1999**, *70*, 2606–2614.
- (24) Powers, D. E.; Hansen, S. G.; Geusic, M. E.; Pulu, A. C.; Hopkins, J. B.; Dietz, T. G.; Duncan, M. A.; Langridge-Smith, P. R. R.; Smalley, R. E. *J. Phys. Chem.* **1982**, *86*, 2556–2560.
- (25) Levine, R. D.; Bernstein, R. B. *Molecular Reaction Dynamics and Chemical Reactivity*; Oxford University Press: Oxford, U.K., 1987.
- (26) (a) Miller, W. B.; Safron, S. A.; Herschbach, D. R. *Discuss. Faraday Soc.* **1967**, *44*, 108–122. (b) Miller, W. B.; Safron, S. A.; Herschbach, D. R. *J. Chem. Phys.* **1972**, *56*, 3581–3592.
- (27) The actual uncertainty in the threshold for fitting the data was ± 0.5 kcal/mol, but we cannot distinguish whether the YC_4H_4 products resulted from the ground spin–orbit state $Y(a^2D_{3/2})$ or the excited spin–orbit state $Y(a^2D_{5/2})$, lying 1.5 kcal/mol higher in energy. We therefore increased the error bars to ± 2.0 kcal/mol to include this uncertainty.
- (28) Stauffer, H. U.; Hinrichs, R. Z.; Schroden, J. J.; Davis, H. F. *J. Chem. Phys.* **1999**, *111*, 10758–10761.
- (29) Schroden, J. J.; Teo, M.; Davis, H. F. *J. Chem. Phys.* **2002**, *117*, 9258–9265.
- (30) (a) Bayse, C. A. *J. Phys. Chem. A* **2002**, *106*, 4226–4229. (b) Schroden, J. J.; Davis, H. F.; Bayse, C. A. *J. Phys. Chem. A* **2007**, *111*, 11421–11429.
- (31) This value was estimated by increasing the binding energy by 5 kcal/mol over that for the Sc–benzene complex¹⁹ because Y typically forms stronger bonds with hydrocarbons than Sc.
- (32) Dinadayalane, T. C.; Priyakumar, U. D.; Sastry, G. N. *J. Phys. Chem. A* **2004**, *108*, 11433–11448.
- (33) Siegbahn, P. E. M. *Theor. Chim. Acta* **1994**, *87*, 277–292.